

EXPERIMENTAL STUDY OF BEARING CAPACITY EFFECT IN SWELLING SOIL

A.N. MOHAMMED and A.A. KHALIL*
University of Mosul, Department of Civil Eng., IRAQ
E-mail: amina.alshumam@uomosul.edu.iq

The current study aims to investigate the effects of swell pressure on the bearing capacity of swelling soil. A model and some laboratory tests have been created to investigate the swell pressure effect on the bearing capacity variation of soil swelling due to swelling pressure. The influence of varying water content w/c and dry unit weight (γ_d) on the shear strength and swelling pressure was studied. The soil has been taken from Diwan Residential Compound-Mosul. It is classified as highly swelling soil. The swell pressure of soils at their natural water content reached 385 kN/m^2 . Experiment results show that the parameters of shear resistance decreased with the w/c increase at the constant value of (γ_d), and increased with the (γ_d) increase when the w/c was constant. Results show that the swelling pressure decreased with the w/c increase, while it increased with the (γ_d) increase. Also, the results obtained using was model show that the resistance of bearing capacity of pre-saturated selected soil was 196 kN/m^2 , while the bearing capacity was 620 kN/m^2 when taking into account in the generation of swelling pressure.

Key words: swell pressure, swelling soil, bearing capacity, water content, dry unit weight.

1. Introduction

The swelling soil spreads in many different areas in Iraq with uneven degrees of expansion, that starts with low expansive to high expansive. It spreads widely in the middle and northern Iraq [1]. As a result, many problems have appeared in different lightweight structures set up on this soil [2, 3].

The swelling soil has been observed in Mosul city with different swelling degrees in many places in the left bank at Al-Kafaat, Al-Kindy, Al-Hadbaa, some parts of al-Zuhur, Al Sedeeq, Hayy Al-Jami'a, Al-Arabi and al-Wahda. In the right bank of Mosul, the swelling soil exists in al-Yarmouk, some places of al-Thawra, al-Mawsil al-Jadidah, and al-Rifai. This has led many researchers to study the expansive soil in Mosul. The reason behind the damages that are inflicted to the lightweight structures may be due to the volume changes that the swelling soil is exposed to [4]. The different properties of expansive soil have a great role in soil structure, w/c , and (γ_d) because of their minerals [5]. The hydrophilic minerals are considered one of the most important characteristics that affect the shear strength of the soil. Expansive soils are strenuous and have a high value of shear strength when they are dry, while they lose these characteristics whenever the moisture increases. Additionally, seasonal temperature changes in w/c have a significant effect on the shear strength value of this soil [4]. So, the w/c change of the expansive soil leads to high changes in the size of the expansive soil, which can cause high swell pressure that leads to damage in the lightweight structures [6].

Most of the studies that have been used to measure the bearing capacity of swelling soil assume that the soil is in a saturated case with local shear failure, which leads to a reduction of the values of the shear resistance parameters

* To whom correspondence should be addressed

in the saturated case [7]. A lot of researchers have conducted different studies in which they have found that the swell pressure of the expansive soil depends on the moisture content and dry density.

Al-Mhaidib and Al-Shamrani [8] studied the influence of swell pressure on the shear strength of the swelling soil. They used models that were prepared with constant initial (γ_d) and various w/c . It was observed that swelling has a significant influence on the shear strength. Xiao and Wang [9] conducted a study in which they made a direct shear test and a swelling test on undisturbed samples to study the influence of w/c on the shear strength and swell pressure. It was found that the shear strength coefficients and the swell pressure of the soil decrease with the w/c increase.

Farzad and Hamid [10] conducted a study on a group of models of undisturbed swelling soil to investigate the influence of the initial w/c on the untrained shear strength of the swelling soil. The results show that the shear strength of the swelling soil is dependent on the confining pressure and the initial w/c of the models. The shear strength is decreasing with the increase of the initial moisture content.

Vilas and Moniuddinmd [11] conducted a study to identify the bearing capacity of the high swelling soil using the finite element method. The theoretical results were compared with the traditional theoretical results. The results obtained from the numerical analysis are the closest to results of Terzaghi's equation.

Paul and Aaron [12] investigated the values of the shear strength and bearing capacity by using Plaxis and compared the results obtained by Terzaghi, Hansen, and Meyerhof's equations. The results show that (γ_d) values are close to the values that have been obtained using the above equations. Abid [13] conducted a study that aims at investigating the influence of swell pressure on the bearing capacity of the swelling soil for three kinds of soils that have been taken from three different areas in Syria by using a laboratory model of square footing to identify the bearing capacity of the selected soil through applying an increased loading on a footing for two cases, using a loading arm until failure. The results showed that the swell pressure related to the initial moisture and dry density increased the bearing capacity of the swelling soil.

To achieve the aim of the present study the effect of swell pressure on the bearing capacity of the expansive soil has been studied by using a laboratory model. The obtained results show that the swell pressure affected the bearing capacity values of the expansive soil. Also, many laboratory tests have been conducted to study the difference of shear strength and swell pressure coefficients of the swelling soils with the change of the initial w/c and (γ_d).

2. Materials and methods

2.1. The soil

The soil that has been used in this study was selected from al-Arabi-Diwan Residential Compound/Mosul (site coordinate is 36°24'54.3"N 43°06'58.9"E).

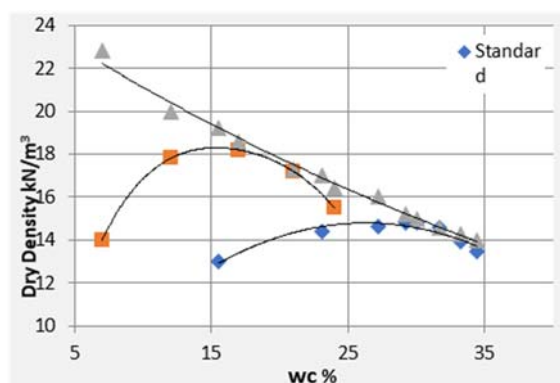


Fig.1. Compaction curves.

The samples were taken from 2 to 2.5m depth, the soil was shale with brown color, and it is classified as high plasticity clay soil. The reason for choosing this soil is that there are many problems in the buildings, such as cracks on the walls of the buildings. Table 1 shows the soil physical characteristics. The soil compaction characteristics (by using standard and modified compaction effort), and the grain size distribution analysis are illustrated in Figs 1 and 2, respectively.

Table 1. Physical characteristic of soil.

Description		Value
Liquid Limit		73 %
Plastic Limit		38 %
Plasticity Index		34 %
Linear Shrinkage		17.64 %
Water Content		26 %
Specific Gravity		2.72
Sand		8 %
Silt		36 %
Clay		56 %
Unified Soil Classification System		High plasticity clay soil
Standard Compaction	Maximum dry density (kN / m^3)	14.48
	O.M.C	29 %
Swell Pressure		385kN / m ²
Free-Swell		2.2%

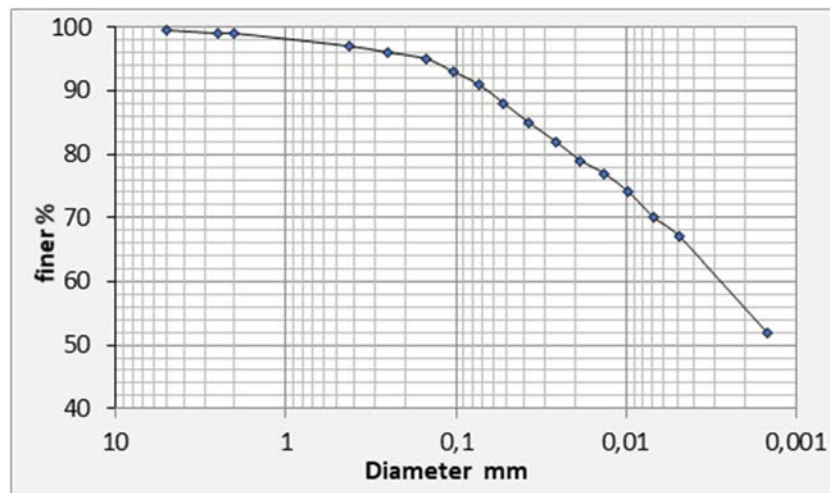
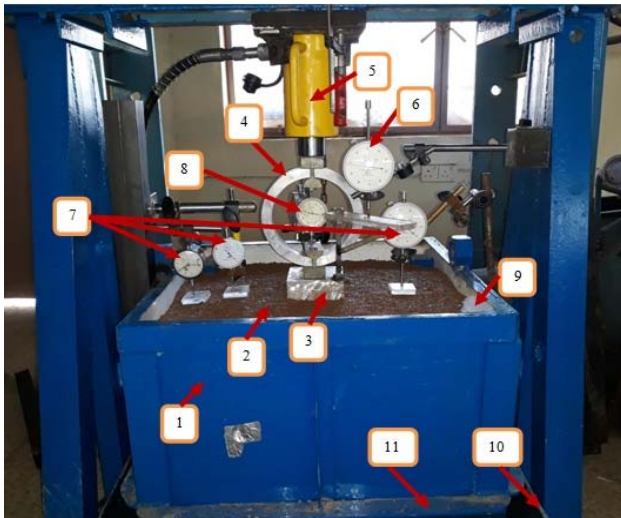


Fig.2. Grain size distribution.

2.2. The model used in this study

A laboratory model was made of dimensions ($0.55 \times 0.55 \times 0.65m$). The model was supported from outside with stainless steel bars ($0.1 \times 0.1 \times 0.035m$), with a loading system consisting of a two-iron columns ($90 \times 90cm$), and a (10 ton) ring attached from the top to a hydraulic jack (20 ton) capacity, the foundation was

placed at the center with two dial gauges with accuracy (0.01mm) at the opposite corners to record displacement details, to obtain an adequate perception of the expansive soil behavior during the test, dial gauges (0.01mm) were installed at 2B from the base edge to ensure practically that no effect occurred at the edge of the box as shown in Fig.3.



1. The test box at ($0.55 \times 0.55 \times 0.6\text{ m}$)
2. The Soil Mass.
3. Solid foundation with ($0.1 \times 0.1 \times 0.35\text{ m}$).
4. Proving ring.
5. Hydraulic jack
6. dial gauges used to measure landing details.
7. dial gauges used to show the deformation of soil.
8. dial gauges used to measure the direct loading.
9. Water supply system.
10. The saturation pan.
11. Filter.

Fig.3. Model details used in study.

The soil saturation system adopted in four perforated tubes installed in the four corners of the box, to achieve the optimal distribution of water within the soil mass in the box and to ensure soil saturation and also to saturate the soil from below by placing the box containing the soil mass formed into a water saturation pan of dimensions ($0.6 \times 0.6 \times 0.75\text{ m}$). Figure 4 shows a cross-section detailing the saturation system used in the study.

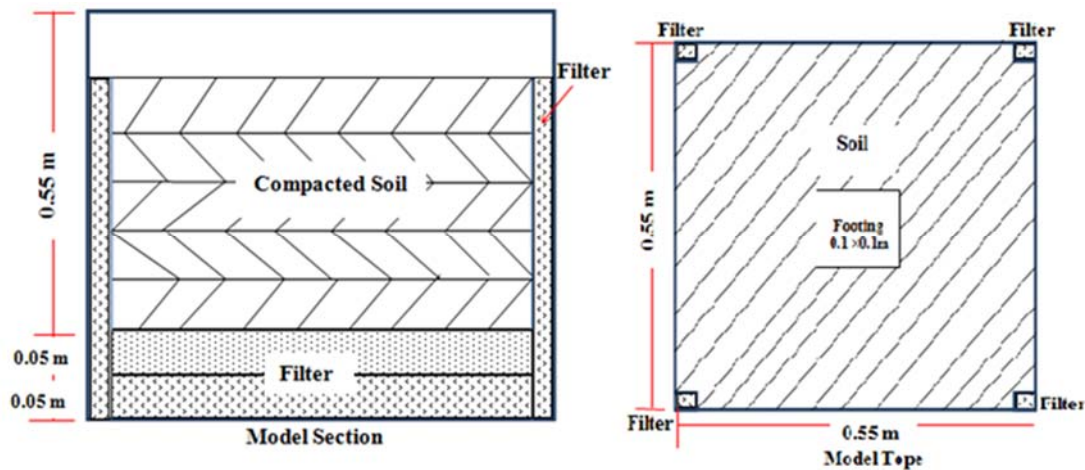


Fig.4. Cross-section detailing the saturation system used in model study.

The model soil sample was prepared by fragmenting the soil sample, which was taken from the field, then this soil was passed through (4.75mm) sieve and was dried. The soil was mixed with specific quantities of water to get the moisture content required. After that the soil was left for five days in plastic bags. According to the method described by Agus *et al.* [14], Vanapalli and Taylan [15]. Then the soil was compacted in a test box into layers with a thickness of (0.1 m) for each layer by using a compactor device prepared for this purpose

with a capacity of (80) and internal dimensions ($1 \times 1 \times 1m$). A hydraulic piston with a cylindrical piston crane ($0.11m$) in diameter and ($0.90m$) in length was used. An oil material was placed on the sides of the model to reduce friction between the model and soil layers (Tsukamoto *et al.* [16]). Also, a ($10cm$) thickness filter layer was placed at the base of the box to ensure that water reaches the soil mass. The soil used in the model had moisture content (17.18%) and dry density ($13.76kN/m^3$), which is equivalent to 95% of the dry density. Several readings were taken for both the w/c and the (γ_d) of the soil at different depths. Table 2 shows the values of moisture content and dry density of the soil within the model.

Table 2. Moisture content and dry density variation with depth.

Depth m	Moisture content %	Dry density KN/m^3
0.1	17.14	13.73
0.2	17.12	13.76
0.3	17.2	13.7
0.4	17.25	13.69
0.5	17.22	13.72
average	17.18	13.72

We studied two cases: in the first case soil was laid to be saturated within the box and after the saturation was completed a square footing with dimensions ($0.1 \times 0.1 \times 0.25cm$) was placed on the soil surface. Then the process of loading began, each load was left for 24 hours or till obtaining three equal readings, then the load applying continued until the permissible settled value ($25mm$) was reached. In this case (pre-saturated soil condition) the swell pressure was not measured. Dial gauges were used for taking footing displacement and then the loading process started until failure occurred. It was confirmed that the soil reached saturation status by dial gauges installed on the soil surface and monitoring of soil surface swelling as well as the extraction of soil models to determine the moisture content through side openings in the box prepared for this purpose. In this case, the shear strength of the swelling soil was determined without taking into consideration the swell pressure (Fig.5.).

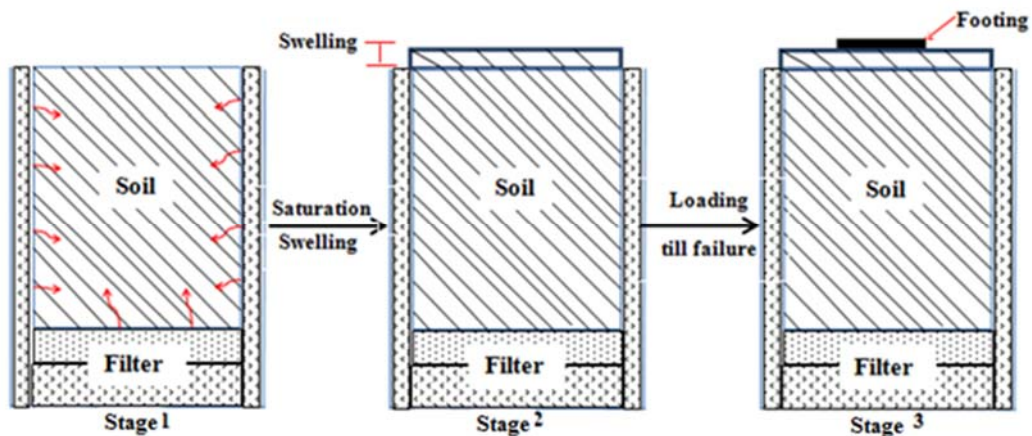


Fig.5. Details of the first stage of the model test.

For the second case, the soil was prepared with the same (w/c) and (γ_d) as in the first case. Then the soil was saturated after additional loads were applied till the soil failed. It was supposed that soil failure would occur at the load equivalent to the failure load in the first case, but the soil continued to resist the applied load.

Through this test, the value of shear strength of the soil taken into consideration and the swell pressure have been obtained. Figure 6 shows the second stage of the model case.

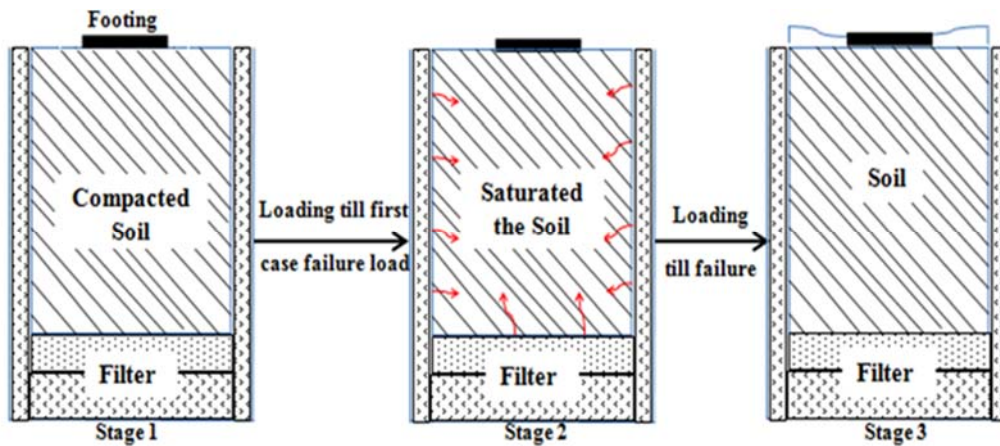


Fig.6. Details of the second stage of the model test.

3. Results

The effect of the w/c on the values of shear strength parameters (cohesion) studied at constant values of (γ_d) are shown in Tab.3.). From the results it is clear that the cohesion values decrease with (15%, 60%) with the w/c values increased for (γ_d) values (13.7 and 15.69kN/m³) respectively.

Table 3. Cohesion values at constant dry density and variable moisture content.

moisture content %	Cohesion kN / m^2	
	$\gamma_d = 13.73kN / m^3$	$\gamma_d = 15.69kN / m^3$
17	31.97	86.088
20	28.76	82.132
22	24.19	79.562
24	23.405	76.524
26	23.054	72.982
28	22.228	-
30	20.79	-
32	12.749	-

Table 4 illustrates the results of the angles of friction for w/c values change at (γ_d) (13.7, and 15.69 kN / m³). It is noted that there is a decrease of angles of friction values (18.2%, 20.9%) if the w/c values increase for selected values of (γ_d) (13.73 and 15.69kN / m³). This result agrees with the conclusion of Wang *et al.* [17].

Table 4. Angle of internal friction values at constant dry density and variable moisture content.

moisture content %	angle of internal friction	
	$\gamma_d = 13.73 \text{KN} / \text{m}^3$	$\gamma_d = 15.69 \text{KN} / \text{m}^3$
17	28.3	39.7
20	28.15	37.3
22	27.6	34.9
24	27.3	32.7
26	27	31.4
28	26.8	-
30	25	-
32	23.3	-

This case illustrates that there is an inverse relation among these values as represented in equations (3.1) and (3.2) stated below. Each of the values (c, ϕ) shown in Eqs (3.1) and (3.2) can be compensated in the Terzaghi general equation of bearing capacity.

$$c = 34.26 + 0.245\omega - 0.026\omega^2, \quad (R^2 = 0.865), \tag{3.1}$$

$$\phi = 57.21 - 1.062\omega + 0.002\omega^2, \quad (R^2 = 0.992). \tag{3.2}$$

The effect of (γ_d) on shear strength parameters values at constant w/c are shown in Tabs 5 and 6. The cohesion values increase with the increased (γ_d) with the constant w/c . The relation between changing each of the (γ_d) and shear strength parameters at ($\gamma_d = 13.73 \text{kN} / \text{m}^3$) and ($w/c = 17\%$) can be expressed in Eqs (3.4) and (3.5) which illustrate that there is a good relationship between these values:

$$c = -692.8 + 73.52\gamma_d - 1.549\gamma_d^2, \quad (R^2 = 0.924), \tag{3.3}$$

$$\phi = -280.1 + 37.03\gamma_d - 1.056\gamma_d^2, \quad (R^2 = 0.919). \tag{3.4}$$

Table 5. Cohesion values at variable dry density and constant moisture content.

$\gamma_d [kN / m^3]$	W%	17%	20%	22%	24%	26%	28%	30%	32%
	Cohesion (kN / m^2)								
13.73		31.97	28.76	24.19	23.41	23.05	22.23	20.79	12.75
15.69		86.10	82.13	79.56	76.52	72.98	-	-	-

Each of the values (c, ϕ) shown in Eqs (3.4) and (3.5) can be compensated in the Terzaghi general equation of bearing capacity. Then, this equation will refer to (γ_d) in a way that it can be applied within the

range of soil features under study with range $(15.69, 13.73kN / m^3)$ of (γ_d) . In the previous equations, the value of (w) used as a percentage value $(\gamma_d [kN / m^3])$ is substituted by values $(C [kN / m^2])$ and $(\phi [deg])$.

To study the influence of changes in the w/c on the swell pressure at constant (γ_d) , a swell pressure (fixed size) was carried out for disturbed samples, and the models prepared at different values of w/c ranged between $(17\% \text{ to } 32\%)$ for three values of (γ_d) $(11.7, 13.7 \text{ and } 15.7kN / m^3)$. Figure 7 shows the results of the test.

Table 6. Angle of internal friction values at a variable dry density and constant moisture content.

$\gamma_d [kN / m^3]$	W%	17%	20%	22%	24%	26%	28%	30%	32%
	angle of internal friction								
13.73		28.5	28.15	27.6	27.3	27	26.8	25	23.3
15.69		39.7	37.3	34.9	32.7	31.4	-	-	-

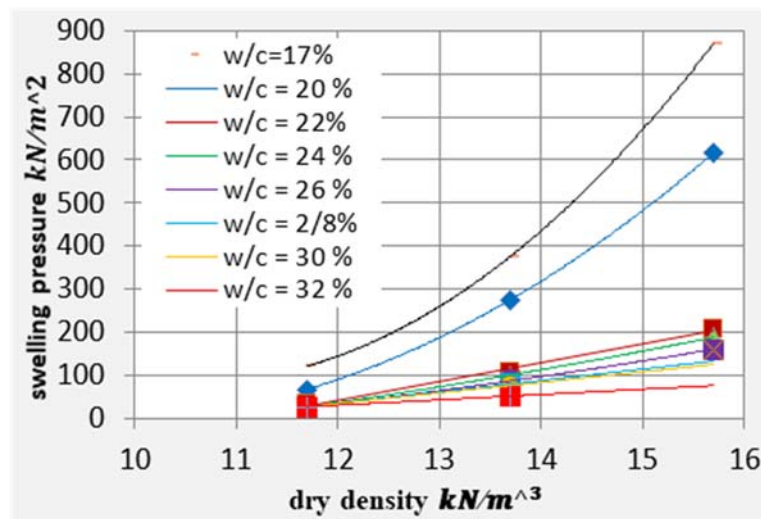


Fig.7. Swell pressure relation with the initial moisture content.

Figure 8. shows the effect of (γ_d) change on the swell pressure, obtained for the models laid down was at initial (γ_d) $(15.69kN / m^3; 870.72kN / m^2)$ and the lowest swell pressure obtained was an initial (γ_d) $(11.7kN / m^3)$ with $(27.58kN / m^3)$.

It is essential to note that the main objective of the study was to investigate the influence of both w/c and (γ_d) changes on shear strength parameters and swelling pressure that was presented and discussed for the soil of the selected area, also for expansive soil with similar characteristics or approach to the w/c or (γ_d) for soil chosen, and to obtain laboratory results, which can be used in theoretical equations that enable us to

guess the bearing capacity of the swelling soil at this range of characteristics taking into account the value of swell pressure in these equations as an impact factor.

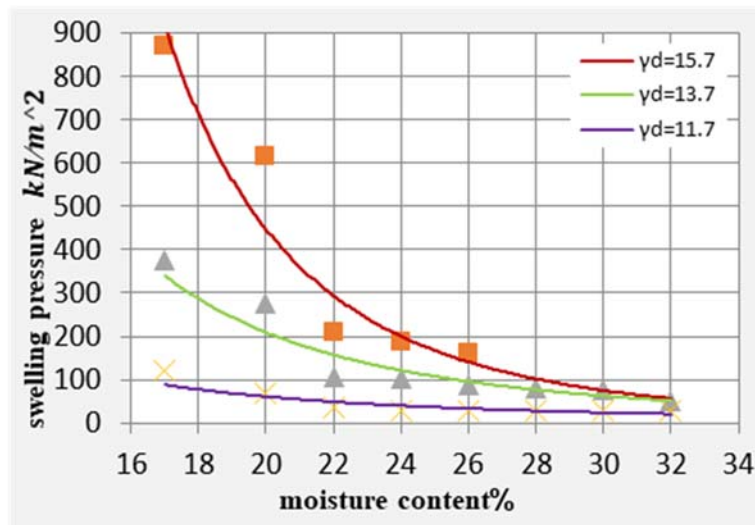


Fig.8. Swell pressure relation with dry density.

To determine the bearing of expansive soil and how it can be affected by the presence of water, two tests were made to find the bearing capacity of the soil: the first test consisted in measuring the bearing capacity of the soil when saturated, while the other in measuring the bearing capacity of the soil exposed to pre-pressure equal to the value of the pressure causing failure in the first case without saturating the model and then saturating the model and continued loading soil till failure.

Figure 9 shows the relationship between stress and displacement at failure load for both cases. It is not that the soil failed at load ($\sigma_{sat} = 196 \text{ kN} / \text{m}^2$) in the first case, while it failed at the second case at a larger load. It failed at the first case with the value of $\sigma_{sat.sw.} = 620 \text{ kN} / \text{m}^2$. The difference between shear strength taking into account the effect of the swell pressure and shear strength without measuring the swell pressure represents the effect of the swell pressure on the shear strength of the swelling soil $\Delta\sigma$.

Table 7. Variables and bearing capacity values calculated.

swelling pressure	R	w/c	γ_d kN / m ³	γ_m kN / m ³	C kN / m ²	ϕ	σ_{case1} (kN / m ²)	σ_{case2} (kN / m ²)
0	1	-	-	-	-	-	-	-
376	3.2	17.17	13.7	16	31.9	28.5	620	196
107.2	1.37	22	13.7	16.8	24.2	28.1	381	277
101.1	1.38	24	13.7	17	25.2	27.3	379	273
87.3	1.4	26	13.7	17.3	23.1	27	376	266
80.4	1.38	28	13.7	17.6	22.22	26.8	364	263
76.6	1.35	30	13.7	17.9	20.79	25	347	256

To obtain a relation presenting the effect of the swell pressure the general bearing capacity equation which gives a primary impression of the bearing capacity of expansive soil in the range of (w/c) and (γ_d)

must be added. Results of the laboratory model with two previous cases under the same variables of the laboratory model at 13.7 kN/m^3 for (γ_d) and the extent of w/c (22%–30%), which is within the range of the w/c , ϕ the angle of internal friction and cohesion values shown in Tab.7.

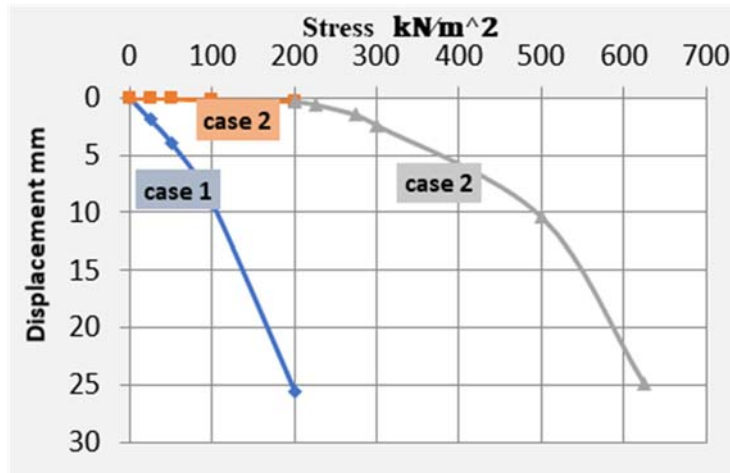


Fig.9. Relationship between stress and displacement.

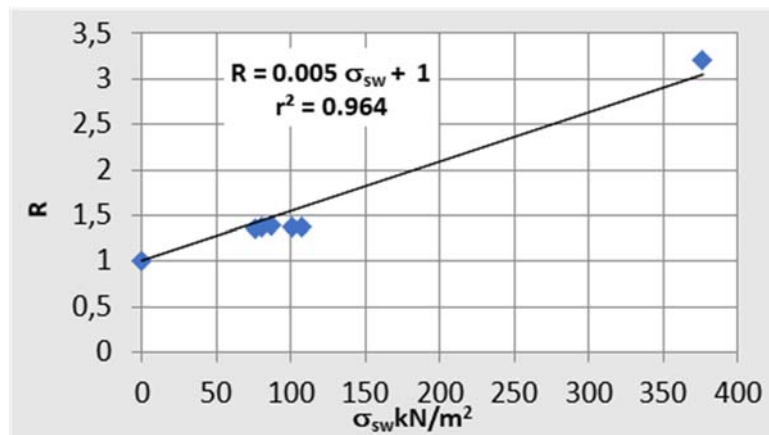


Fig.10. Relation between ratio R and swelling pressure (σ_{sw}).

Figure 10 presents the relation between the swell pressure (σ_{sw}) obtained from the experiments by using the odometer test and R-value which is equal to the ratio between the bearing capacity with and without the presence of the swell pressure ($\sigma_{sat.sw}$ and σ_{sw}). We note linear relationship ratio between (R) and swell pressure, this can be clarified in Eq.(3.7). It is noticed that the values of the failure loads obtained for the pre-saturation state are close to the bearing capacity calculated from the Terzaghi equation that is equal to (234 kN/m^2). It ranged between (15.5%-16.2%) for the selected angle of friction range (25-28.5).

$$R = 0.0054 \sigma_{sw} + 1, \tag{3.5}$$

$$R = \frac{\sigma_{sat.sw}}{\sigma_{sat}}. \tag{3.6}$$

So:

$$\sigma_{sat.sw} = \sigma_{sat} \times (0.0054\sigma_{sw} + 1) \quad (3.7)$$

where $\sigma_{sat.sw}$ is the bearing capacity of the soil taking the effect of the swell pressure, σ_{sat} is the bearing capacity of the soil according to the equation prepared by Terzaghi, and (R) is the influence of the swell pressure. The equation above enables us to find the bearing capacity of a square footing placed on the swelling soil taking into account the effect of the swell pressure. Applying Eq.(3.7) requires that the values (C, ϕ) calculated from direct shear testing (UU) at a w/c are (22%-30%), and for (γ_d) close to $(13.7kN / m^3)$.

4. Conclusions

The following conclusions from this research study could be drawn:

1. There is no influence of the swell pressure on the shear strength of the swelling soil if the footing is implemented after saturation, as the value of the shear strength in this case is $(\sigma_{sat} = 196kN/m^2)$.
2. The swell pressure increases the shear strength of the swelling soil in the event of performing the foundation before pre-saturation of the soil

Nomenclature

w/c	– water content
(γ_d)	– dry unit weight
σ_{sat}	– bearing capacity of pre-saturated selected soil
$\sigma_{sat.sw}$	– swelling pressure
c	– cohesion
ϕ	– angle of internal friction
r^2	– square root of the equation
R	– influence of swell pressure
UU	– unconsolidation-undrain shear test

5. References

- [1] Al-Sayegh S.K. (1988): *Swelling Characteristics of the Soil of the City of Erbil*.– M.Sc. Thesis, Faculty of Engineering, Salah Al-Din University.
- [2] Al-Sanjari Othman Abdul-Karim Nasser (1997): *Study of Some Swollen Properties of the Soil of the City of Mosul (Al-Kafaat Al-Thaniyah District)*.– Master Thesis, College of Engineering, Salah Al-Din University.
- [3] Sabbbah M.R, (1987): *Evaluation of Soil Properties in Middle Part of Iraq*.– M.Sc Thesis, Dept.of Building and Construction Engg., University of Technology, Baghdad, Iraq.
- [4] Hazim A.A. and Khalil A.A. (2019): *Effect of Water Seepage on the Volume Change of Expansive Soil under Light Weight Buildings' Foundations (in Arabic)*.– M.Sc. Thesis, Mosul University, Iraq.
- [5] Al-Obaydi M.A., Al-Kiki I.M. and Aldaood A.H. (2019): *Effect of swelling on the shear strength behaviour of expansive soil*, International Journal of Geotechnical Engineering, DOI: 10.1080/19386362.1651043.
- [6] Zheng S., Daokun Q., Xinju G., Xiaojuan X. and Lianzhang Z. (2018): *Characterization of the undrained shear strength of expansive soils of High water content*.– MATEC Web of Conferences vol.206, Article No.01002. DOI: 10.1051/mateconf/201820601002.

- [7] Terzaghi K. and Peck R. (1967): *Soil Mechanics in Engineering Practice.*– John Wiley, New York.
- [8] Al-Mhaidib A.I. and Al-Shamrani M.A. (2006): *Influence of swell on shear strength of expansive soils.*– Geotechnical Special Publication, Paper No.ISRM-IS-2000-204. DOI: 10.1061/40860(192)16.
- [9] Xiao W. and Wang Z.-R. (2017): *The relationship between the swelling pressure and shear strength of unsaturated soil: the Yanji Basin as a case study.*– Arabian Journal of Geosciences, vol.10, No.15, Article No.330.
- [10] Habibbeygi F. and Nikraz H. (2018): *Characterization of the undrained shear strength of expansive clays at high initial water content using intrinsic concept.*– International Journal of Geomate, vol.14, pp.176-182.
- [11] Vilas M.R. and Moniuddin K. (2015): *Finite element analysis of soil bearing capacity using plaxis.*– International Journal of Engineering Research and Technology, vol.4, No.6. Doi: 10.17577/IJERTV4IS060813.
- [12] Akagwu P. and Aboshio A. (2016): *Failure modes and bearing capacity estimation for strip foundations in C- ϕ soils: a numerical study.*– World Academy of Science, Engineering and Technology International Journal of Civil and Environmental Engineering, vol.10, No.9, pp.1228-1232.
- [13] Abed A. (2003): *The effect of soil swelling pressure on bearing capacity.*– M.Sc. Thesis, Al-Baath University, College of Civil Engineering.
- [14] Agus S.S., Schanz T., Fredlund D.G. (2010): *Measurements of suction versus water content for bentonite – Sand Mixtures.*– Geotechnical Testing Journal, vol.126, No.2, pp.179-190.
- [15] Vanapalli S.K. and Taylan Z.N. (2012): *Design of single piles using the mechanics of unsaturated soils.*– International Journal of GEOMATE, vol.2, No.1, pp.197-204.
- [16] Tsukamoto Y., Ishihara K., Higuchi T. and Aoki H. (1999): *Influence of geogrid reinforcement on lateral Earth pressures against model retaining walls.*– Geosynthetics International, vol.6, No.3, pp.195-217.
- [17] Wang L.-C., Long W. and Gao S.-J. (2014): *Effect of moisture content, void ratio and compacted on the shear strength of remoulded unsaturated clay.*– EJGE, vol.19, pp.4413-4426.

Received: May 28, 2021

Revised: October 11, 2021